

# Structure transformation in graphite at high-energy ball milling treatment

Inna Kirian, Alexander Rud, Andrey Lakhnik

G.V. Kurdyumov Institute for Metal Physics N.A.S. of Ukraine, Kyiv, Ukraine

kiryan.inna@gmail.com

**Abstract:** The changes in the structure of the crystalline graphite are studied during high-energy ball milling (BM) treatment. It was found by XRD analysis the milling time increasing up to 3.5 h leads to the formation of an amorphous phase in the milling process. After 10 h of ball milling treatment, complete amorphization of graphite takes place. It has been shown by high-resolution electron microscopy the individual particles have complex morphology which depends on the BM time. After 1 h of BM carbon materials characterized by an onion-like structure: the individual particles have a spheroidal shape with a size of ~ 10 nm. However, unlike the previous ones after 10 h of ball milling carbon nanomaterials are characterized by a disordered structure, which is typical for amorphous carbon.

**Keywords:** GRAPHITE, ONION-LIKE, BALL-MILLING, XRD, MICROSTRUCTURE

## 1. Introduction

The attention to carbon has been focused for a long time due to a broad spectrum of allotropic modifications depended on the degree of  $sp$ -hybridization of valence electrons [1-4]. Under the classification scheme of Heimann and coworkers [5], the basic forms of carbon allotropes are diamond, graphite and carbene with integer degrees of bond hybridization  $sp^3$ ,  $sp^2$  and  $sp$ , respectively. The new spatial forms of carbon (fullerenes and nanotubes) have non-integer degrees of bond hybridization  $sp^{2+x}$  ( $x < 1$ ). A broad class of disordered carbon materials related to transitional carbon is in the center of the scheme. These substances (amorphous carbon, soot, vitreous carbon, diamond-like carbon, carbon spheres, cokes, coals, etc.) consist of randomly arranged carbon atoms at the different hybridization states [5]. Due to the unique physical, chemical, and mechanical properties carbon nanomaterials are extensively used in the industry and are very promising in the future, also.

The amorphous carbon can be easily produced by either high-energy ball-milling (BM) of graphite [6, 7] or high-voltage electric discharge treatment of hydrocarbon precursors [8, 9]. There are a large number of methods for the synthesis of onion-like carbon materials. The heat treatment and electron beam irradiation of nano-diamonds are most extensively used [10, 11]. The first method consists of the formation of onions due to the heating of pre-obtained ultrafine diamonds. The formation of ions takes place by graphitization of the nano-diamond. This process begins on the surface and spreads to the center of the particle. As a result of heat treatment, the graphite layers are curved and closed, forming nested fullerene-like shells. Since nano-diamonds tend to form agglomerates, a joint shell for several ions can be formed at the junctions of particles as a result of the diffuse mobility of carbon atoms under the action of temperature. In our previous work, the onion-like structure was synthesis by high-frequency electric discharge treatment of propane-butane [12].

In this work, we investigate the formation of different carbons allotropic forms during ball mill treatment of crystalline graphite.

## 2. Materials and methods

Crystalline spectrally pure graphite powder (99.99 % C) was used as the starting material. Graphite samples were milled on the Fritsch Pulverisette P-6 laboratory planetary mill in argon gas atmosphere at room temperature for 0.5, 1, 2, 3.5, and 10 hours, respectively. The sample weight, the rotational speed of the vial (400 rpm), the amount of the steel balls (20 mm; 15), and the ball-to-powder ratio (30:1) were kept in all experiments. Every 5 min of milling was followed by the 5 min of standby. Then milling process was continued with the reverse vial rotation. All samples were handled and stored in the small containers in the glove box filled with purified argon (99.998%) to prevent the powders from oxidation.

X-Ray data were collected using a standard powder diffractometer with monochromatic  $Mo-K_{\alpha}$  radiation (primer pirographite monochromator). The experimental structure factors and the radial distribution functions are calculated by the procedure described in [13, 14]. Electron microscopy investigations were

performed on the high-resolution microscope JEOL JEM-2100F and scanning electron microscope JEOL JSEM IT-500. Raman spectroscopy was performed on Horiba Jobin-Yvon T64000 spectrometer ( $\lambda = 514$  nm) at room temperature.

## 3. Results and discussion

The XRD patterns of the graphite samples after ball milling for different times are shown in Figure 1. The intensive peak at  $12.2^{\circ}$  on the XRD pattern is a reflex from the (002) plane of the pristine graphite.

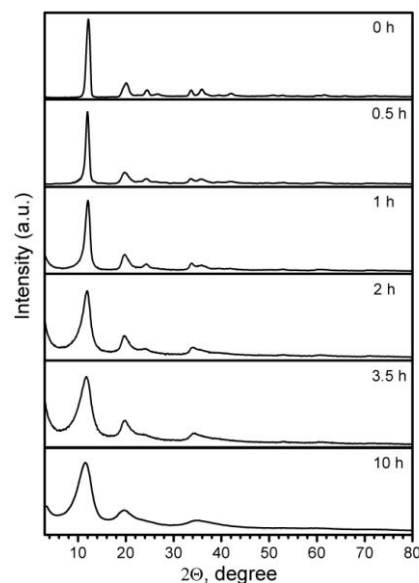


**Fig. 1** The X-diffraction pattern of graphite before and after milling,  $Mo K_{\alpha}$  radiation.

The decreases of intensity and broadening of the diffraction peaks with increasing milling time are observed. It can be due to gradual disorder of the graphite crystal structure and decrease of powders crystallite size. The increasing milling time to 3.5 hours leads to the appearance of a broad asymmetric halo of the (002) peak in the XRD pattern. It indicates the amorphous phase formed in the process of milling. After 10 hours of ball milling treatment, complete amorphization of graphite takes place. The amorphous carbon nanomaterials can be characterized by graphite- and diamond-like short-range order. However, the experimental XRD patterns do not reproduce complete data about the short-range type order that predominate in the structure of amorphous material. From XRD scattering intensities were calculated experimental total structure factors (SF) and radial distribution functions (RDF) (Fig 2).

The first intensive peak  $S_1$  on SF corresponds to (002) interlayer graphite scattering. In the ball milling process of graphite, there is a shift relative to its position and broadening. For crystalline graphite, the first and second peaks in the RDF centers on 1.42 and 2.45 Å,

respectively, which is close to the literature value [14]. The increasing ball-milling time leads to a shift of the first and second peaks on the RDF in the direction of larger values. After 10 hours of milling, the positions of the first and second peaks on the RDF were 1.48 and 2.48 Å, respectively. This indicates a disorder of the crystal graphite structure with increasing grinding time and formation of amorphous carbon nanomaterial with the graphite-like type of the short-range order.

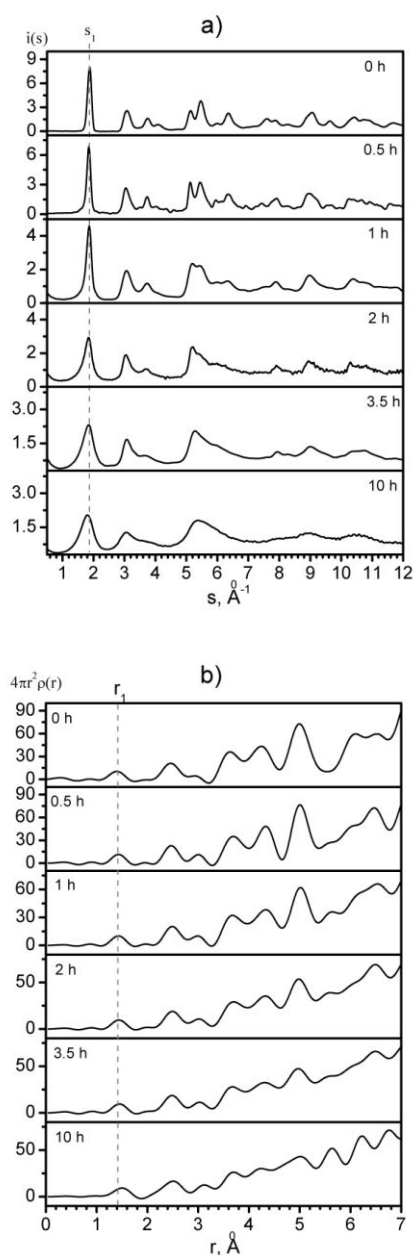


**Fig. 2** Structure factor – (a) and radial distribution functions – (b) calculated from experimental XRD data for pristine and ball-milled graphite.

To clarify the structure of carbon materials individual particles produced by ball-milling of the graphite, high-resolution electron microscopy (HRTEM) was employed. Typical micrographs of carbon nano-materials obtained for 1 and 10 hours of milling are shown in Fig. 3. Carbon nanomaterials obtained after 1 hour of mechanical activation have a complex hierarchical texture and are characterized by an onion-like structure (Fig. 3, b): an individual particle consists of multilayer partially closed defective graphene shells of irregular shape. In the middle of the particle is a disordered nucleus. It is clearly seen that individual particles are collected in agglomerates (Fig. 3, a) and have a spheroidal shape with a size of ~10 nm. However, the graphite powder after 10 hours of MA is

described by the disordered crystal structure, specific for amorphous carbon (Fig. 3, c) in contrast to the samples milled during shorter times. There are diffuse rings visible only and no reflexes on the electronic diffraction pattern (Fig. 3, d). It confirms the amorphous structure was synthesized in the graphite powder after 10 hours of MA. The HRTEM results are in good agreement with the results of the method of radial distribution of atoms.

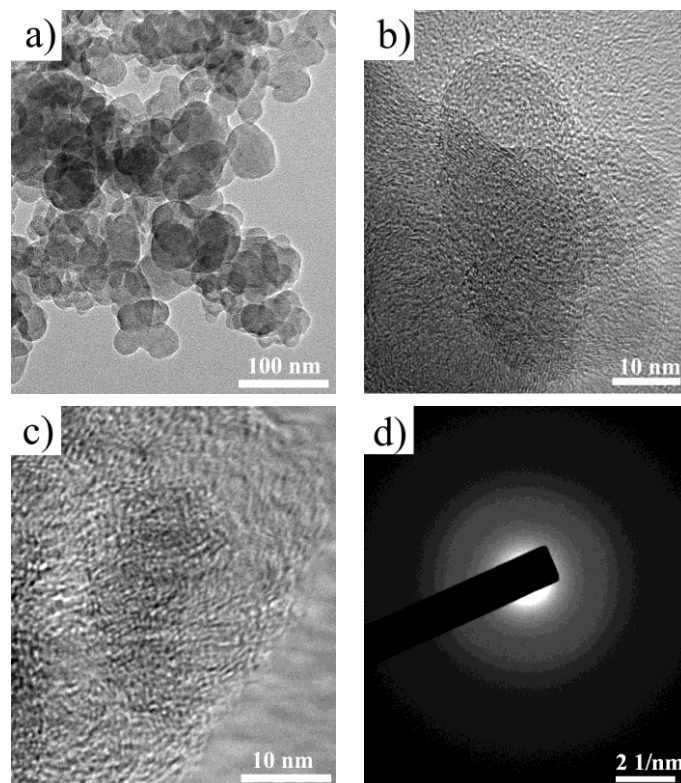


**Fig. 3** Typical microphotographs of carbon nanomaterials obtained after ball mill treatment of graphite: a, b - 1 h, c - 10 h and d - electron microdiffraction for 10 h.

Raman spectroscopy has been applied to analyze carbon materials obtained for the different ball-milling times of crystalline graphite (fig. 4). Raman spectra are characterized by the presence of a G-band, which is shifted towards higher values in the wave vector relative to the tabular one (~1570 cm<sup>-1</sup>) and corresponds to stretching vibrations of atoms with sp<sup>2</sup>-hybridized valence bonds, which are caused by antiphase vibrations of pairs of carbon atoms in various elements structures (rings, chains). Besides the G band, there is an equally intense D-band (the tabular value is ~1350 cm<sup>-1</sup>) in the Raman spectrum. The origin of the D-band is caused by the selection rule due to small ordering regions, various types of defects, and structural disorder. The grinding time increase results in the redistribution in the D- and G- bands intensities. It indicates about the structural disorder in the milled powders. The (I<sub>D</sub>/I<sub>G</sub>)<sup>-1</sup> ratio becomes less due to the decrease in the size of the blocks in the graphene plane. After 1 hour of ball mill processing, the Raman spectrum takes the form typical for carbon nanomaterials. For a detailed analysis of the Raman spectra, the profile of the D and G bands was described by the Pseudo-Voigt function taking into account the background. It is clear the D- and G-bands have different half-widths FWHM (full width at half maximum). The longer the milling time, the more FWHM of the D- and G-bands. The FWHM half-widths of the D- and G-bands are shown in Table 1.

The sizes of the ordered domains  $L_a$  along the basal plane were calculated from the integrated intensities ratio of the I<sub>D</sub>/I<sub>G</sub> bands accordingly to the following equation.

$$L_{(HM)} = \frac{540}{E_1^4} \left( \frac{I_D}{I_G} \right)^{-1},$$

where  $E_1$  is the laser radiation energy.

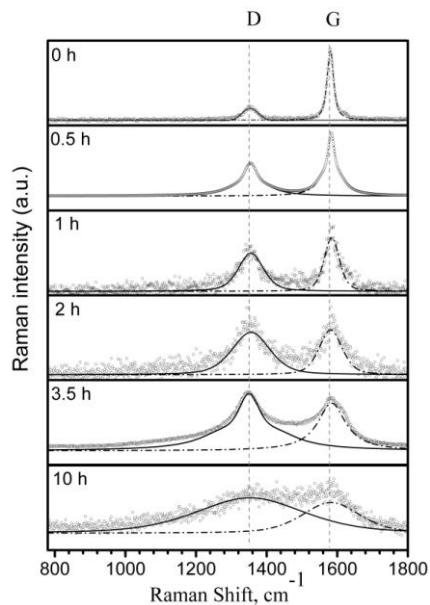


**Fig. 4** The Raman spectra for pristine and ball-milled graphite.

Since a laser with a wavelength of  $\lambda = 514$  nm was used as an excitation source, the energy of laser radiation  $E_1$  in formula (1) is 2.41 eV. The size of the ordered domain decreases for the longer grinding time (see Table 1). So, the studies carried out using Raman spectroscopy showed that the synthesis products are typical amorphous materials, which confirms the results of X-ray structural analysis.

**Table 1:** Value of  $L_a$  ordering regions in the structure of ball-milled graphite.

№	G - band			D - band			$\left(\frac{I_D}{I_G}\right)^{-1}$	$L_a$ , nm
	Centre, $\text{cm}^{-1}$	$FWHM$ , $\text{cm}^{-1}$	$I_G$	Centre, $\text{cm}^{-1}$	$FWHM$ , $\text{cm}^{-1}$	$I_D$		
0h	1580	11	8.42	1353	27	2.13	4	64
0.5h	1583	16	5.42	1354	29	5.05	1.07	17.1
1h	1584	25	8.68	1355	42	1.01	0.86	13.7
2h	1581	38	8.31	1355	63	1.29	0.64	10.2
3.5h	1584	48	5.11	1350	52	8.43	0.6	9.6
10h	1582	96	2.22	1353	180	4.79	0.46	7.4

#### 4. Conclusion

It was shown, graphite crystal structure transforms into an amorphous state during the high-energy ball milling. The carbon powder synthesized by BM has a graphite-like type of the atomic short-range order. As it follows from the HRTEM results, carbon nanomaterials after 1 h of graphite ball-milling of powder has onion-like structure. Carbon powder obtained after 10 hours of BM is characterized by the globular morphology of individual particles with a structure typical to amorphous carbon.

#### 5. Acknowledgement

This work was supported by the National Academy of Sciences of Ukraine youth project № 06/01-2021(03).

#### 6. References

1. A. Krueger, *Carbon materials and nanotechnology* (WILEY-VCH Verlag GmbH and Co. KGaA, Weinheim, 2010)
2. O.A. Shenderova, V.V. Zhirmov, D.W. Brenner, *Crit. Rev. Solid State Mater. Sci.* 27, 227 (2001)
3. E.A. Belenkov, V.A. Greshnyakov, *Phys. Solid State* 55, 1754 (2013)

4. J.T. Wang, C.F. Chen, E.G. Wang, Y. Kawazoe, *Sci. Rep.* 4, doi: 10.1038/srep24665 (2014).
5. R.B. Heimann, S.E. Evsyukov, Y. Koga, *Carbon* 35, 1654 (1997)
6. T. Xing, L.H. Li, L. Hou, X. Hu, S. Zhou, R. Peter, M. Petracic, Y. Chen, *Carbon* 57, 515 (2013)
7. V. Petkov, A. Timmons, J. Camardese, Y. Ren, *J. Phys. Condensed. Matter.* 23, 435003 (2011)
8. L.Z. Boguslavskii, *Surf. Eng. Appl. Electrochem.* 46, 352 (2010)
9. A.D. Rud, N.I. Kuskova, V.Yu. Baklar', L.I. Ivaschuk, L.Z. Boguslavskii, I.M. Kiryan, *State. Bull. Russ. Acad. Sci: Phys.* 75, 1435 (2011)
10. Q. Zou, M.Z. Wang, Y.G. Li, *J. Exp. Nanosci.* 5, 375 (2010)
11. N. Miriyala, D.J. Kirby, A. Cumont, R. Zhang, B. Shi, D. Ouyang, H. Ye, *Cryst.* 10, doi:10.3390/cryst10040281 (2020)
12. A.D. Rud, I.M. Kiryan, *J. Non-Cryst. Solids.* 386, 1 (2014)
13. A.D. Alekseev, G.M. Zelinskaya, A.G. Ilinskii, I.G. Kaban, Yu.V. Lepeyeva, G.S. Mogilny, E.V. Ul'yanova, A.P. Shpak, *Fiz. Tekh. Vis. Davl.* 3, 35 (2008), (in Russian)
14. J. Robertson, *Mater. Sci. Eng. R*, 37, 129 (2002)